## Liquid Crystals

Publication details, including instructions for authors and subscription information:
http://www.informaworld.com/smpp/title~content=t713926090

# Ferroelectric liquid crystals with a thioester linking group positioned at the chiral tail

S. -L. Wu Corresponding author[a]; Z. -L. Yang[a]
[a] Department of Chemical Engineering, Tatung University, 3rd sec., Taipei 104, Taiwan, ROC

**To cite this Article** Wu Corresponding author, S. -L. and Yang, Z. -L.(2004) 'Ferroelectric liquid crystals with a thioester linking group positioned at the chiral tail', Liquid Crystals, 31: 12, 1581 — 1585

**To link to this Article: DOI:** 10.1080/02678290412331286015

**URL:** http://dx.doi.org/10.1080/02678290412331286015

LIQUID CRYSTALS, VOL. 31, NO. 12, DECEMBER 2004, 1581–1585

# Ferroelectric liquid crystals with a thioester linking group positioned at the chiral tail

S.-L. WU* and Z.-L. YANG

Department of Chemical Engineering, Tatung University, 40 Chungshan N. Rd., 3rd sec., Taipei 104, Taiwan, ROC

(*Received 6 February 2004; accepted 24 May 2004*)

A homologous series of chiral thioesters, hexyl (2*S*)-2-[6-(4-alkanoyloxyphenyl)benzoyloxy-2′-naphthyl]thiopropionates, H*n*PBNTP ($n=7$–11) was synthesized, and the mesophases and electro-optical properties were studied. All the materials possess a ferroelectric SmC* phase, which was confirmed by the switching current behaviour. It was found that compounds with a shorter alkyl chain length ($n=7$–9) displayed SmA* and SmC* phases, while, compounds with a longer alkyl chain length ($n=10$ and 11), displayed the SmC* phase exclusively. Spontaneous polarization and apparent tilt angle were also measured. The maximum $\mathbf{P}_s$ values are in the range 15–26 nC cm$^{-2}$, and the maximum $\theta$ values are in the range 23°–28°.

## 1. Introduction

Ferroelectric liquid crystals (FLCs) have been paid much attention as potential materials for display application [1–4]. Many molecules have been designed, synthesized and investigated in order to obtain FLC materials showing a fast response time [5]. Generally, the molecular structure of FLCs consists of a chiral alkyl chain, a core structure and a terminal alkyl chain [6]. It has been found that the incorporation of a thioester in the rigid core, or in a peripheral chain favours the formation of a smectic phase [7–9]. Moreover, a thioester linking group in the molecules could enhance the mesophase thermal stability [7] and polarizability [10], when compared with the analogous carboxylate. Recent studies show that some chiral thioester materials display anitiferroelectric phases [11, 12]. Other studies on the corresponding chiral homologues also show interesting results [13–18].

Our previous results on the study of the chiral ester materials hexyl (2*S*)-2-[6-(4-alkoxyphenyl)benzoyloxy)-2′-naphthyl]thiopropionates, H*m*PBNTP ($m=8$–14) show that these materials favour the formation of smectic phases, SmA* and SmC*; when the achiral alkyl chain length is greater than 12, the SmC* phase is formed exclusively. In order to investigate further, we have investigated the mesomorphic properties of structurally similar chiral thioester materials with an ester group linked to the achiral tail, hexyl (2*S*)-2-[6-(4-alkanoyloxyphenyl)-benzoyloxy-2′-naphthyl]thiopropionates, H*n*PBNTP ($n=7$–11). The general chemical structure for H*n*PBNTP is given below.

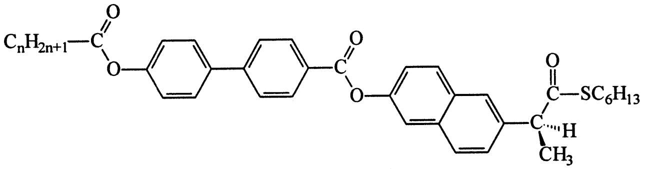

H*n*PBNTP ($n$=7-11)

## 2. Experimental

### 2.1. *Characterization of the chiral materials*

The purity of the final compounds was determined by elemental analysis and the chemical structures were identified by proton NMR using a Bruker WP100SY FTNMR spectrometer.

Transition temperatures and phase transition enthalpies were determined by differential scanning calorimetry using Perkin-Elmer DSC7 calorimeter at a heating rate of 5°C min$^{-1}$. Mesophases were identified by the observation of textures using a Nikon Microphot-FXA optical microscope under crossed polarizers, with a Mettler FP-82 hot stage in conjunction, with a Mettler FP90HT temperature controller.

Electro-optical properties were determined on samples filled in glass cells of 5 μm thickness. The cells were purchased from Linkam Scientific Instruments Ltd, and fabricated by coating with unidirectionally buffed polyimide film. The physical properties of the ferroelectric phase for the materials were measured in antiparallel aligned cells purchased from E.H.C Co.

---

*Author for correspondence; e-mail: slwu@ttu.edu.tw

*Liquid Crystals* ISSN 0267-8292 print/ISSN 1366-5855 online © 2004 Taylor & Francis Ltd
http://www.tandf.co.uk/journals
DOI: 10.1080/02678290412331286015

Japan. The spontaneous polarization ($\mathbf{P}_s$) was measured by a triangular wave method [19] using a frequency of 20 Hz and an amplitude of 5 V.

### 2.2. *Synthesis of the chiral materials*

The chiral materials were synthesized according to procedures illustrated in the scheme.

#### 2.2.1. *Hexyl (2*S*)-2-(6-methoxy-2-naphthyl)thiopropionate, 2*

The chiral acid **1** (5 g, 22 mmol), 1-hexanethiol (2.82 g, 24 mmol), *N,N'*-dicyclohexylcarbodiimide (4.29 g, 24 mmol) (DCC) and 4-dimethylaminopyridine (0.32 g, 2.6 mmol) (DMAP) were dissolved in dry dichloromethane (50 ml) and the solution stirred for 3 days at room temperature. The solid produced was filtered off. The filtrate was washed with 5% acetic acid, aqueous sodium chloride and water. The organic layer was dried over anhydrous magnesium sulphate, concentrated under vacuum and purified by column chromatography over silica gel (70–230 mesh), using dichloromethane/hexane (V/V = 2/3) as the eluent; yield 72%. $^1$H NMR ($CDCl_3$): $\delta$(ppm): 0.84 (t, 3H, $C\mathbf{H}_3$), 1.20–1.53 (m, 8H, $CH_2$), 1.59 (d, 3H, $C^*HC\mathbf{H}_3$), 2.82 (t, 2H, $SC\mathbf{H}_2$), 3.91 (s, 3H, $OC\mathbf{H}_3$ ), 4 (q, 1H, $^*C\mathbf{H}CH_3$), 7.1–7.7 (m, 6H, Ar**H**).

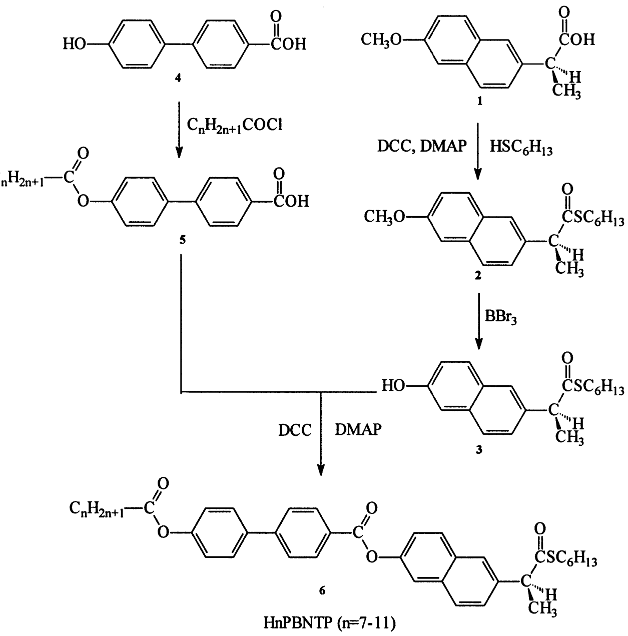

Scheme. Schematic synthetic procedures for H*n*PBNTP (*n* = 7–11).

#### 2.2.2. *Hexyl (2*S*)-2-(6-hydroxy-2'-naphthyl)thiopropionate, 3*

The ester **2** (4.95 g, 15 mmol) was dissolved in anhydrous dichloromethane and the solution cooled to −20°C. Tribromoborane (7.5 g, 30 mmol) was then added, and the mixture was stirred at the same temperature for 10 min, then at 0°C for a further 60 min. The reaction mixture was diluted with dichloromethane (45 ml), and the mixture poured into saturated aqueous ammonium chloride (23 ml) and ice (23 g). The organic layer was separated, washed with saturated aqueous sodium chloride and dried over anhydrous magnesium sulphate. The organic layer was concentrated by evaporation under vacuum. The product was isolated by silica gel (70–230 mesh) column chromatography using dichloromethane as eluent. A resinous product was obtained in 65% yield. $^1$H NMR ($CDCl_3$): $\delta$(ppm): 0.84 (t, 3H, $C\mathbf{H}_3$), 1.20–1.53 (m, 8H, $C\mathbf{H}_2$), 1.59 (d, 3H, $^*CHC\mathbf{H}_3$), 2.82 (t, 2H, $SC\mathbf{H}_2$), 4 (q, 1H, $C^*\mathbf{H}CH_3$), 7.0–7.7 (m, 6H, Ar**H**).

#### 2.2.3. *4-(4'-Alkanoyloxyphenyl)benzoic acid, (*n* = 7–11), 5*

The acid **4** (1.31 g, 6 mmol) and pyridine (5 ml) were mixed in dry dichloromethane (25 ml). Lauroyl chloride (1.34 g, 6 mmol) was dissolved in dry dichloromethane (20 ml) and added to the reaction mixture dropwise, which was then heated under reflux for 3 h and cooled to room temperature. The solution was then acidified with 5% HCl, and the resulting white solid obtained filtered off. The crude products were crystallized from absolute ethanol to yield 80–85% of pure target compounds. $^1$H NMR ($CDCl_3$), typical for **5**($n = 11$): $\delta$(ppm): 0.8–0.9 (t, 3H, $C\mathbf{H}_3$), 1.2–1.5 (m,18H, $(C\mathbf{H}_2)_9$), 2.5–2.6 (t, 2H, $(C\mathbf{H}_2)COO$), 7.1–8.1 (m, 8H, Ar**H**).

#### 2.2.4. *Hexyl (2*S*)-2-[6-(4-alkanoyloxyphenyl)benzoyloxy-2'-naphthyl]thiopropionates HnPBNTP (*n* = 7–11), 6*

The chiral alcohol **3** (0.35 g, 1.1 mmol), acid **5** ($n = 11$, 0.48 g, 1.2 mmol), DCC (0.25 g, 1.2 mmol) and DMAP (0.02 g, 0.12 mmol) were dissolved in dry dichloromethane (50 ml) and the mixture stirred for 3 days at room temperature. The solid produced was filtered and the filtrate washed with 5% acetic acid, 5% aqueous sodium chloride and water. The organic layer was dried over anhydrous magnesium sulphate and concentrated under vacuum. The product obtained was purified by column chromatography over silica gel (70–230 mesh) using dichloromethane/hexane (V/V = 2/3) as eluent. The products were crystallized from absolute ethanol and yielded 80% of pure compound. $^1$H-NMR ($CDCl_3$), typical for **6** ($n = 11$): $\delta$(ppm): 0.85 (dt, 6H, $CH_3$), 1.2–1.6 (m, 24H, $(CH_2)_{12}$), 1.6 (d, 3H, $^*CHC\mathbf{H}_3$), 1.8 (m, 2H, $SCH_2C\mathbf{H}_2$), 2.59 (t, 2H, $SC\mathbf{H}_2$), 2.8 (m,2H, CCH$_2$), 7.2–8.3 (m, 14H, ArH). Elemental analysis data are summarized in table 1.

## 3. Results and discussion

### 3.1. *Mesophase properties*

The phase transitions and corresponding phase transition enthalpies of mesophases for the H*n*PBNTP series were measured by DSC. The mesophases were identified by the observation of microscopic textures under crossed polarizers. The SmA* phase was characterized by the appearance of focal-conic and pseudo-homeotropic textures. The SmC* phase appeared as a striated focal-conic texture and was further characterized by switching current behaviour.

The phase behaviour of H*n*PBNTP ($n=7$–11) is summarized in table 2, and the phase diagram as a function of the alkyl chain length ($n$) on cooling, is plotted in figure 1. The clearing temperatures decrease with increasing terminal chain length, but the SmA*–SmC* transition temperature increases with increasing the terminal chain length. The melting temperature increases until a chain length of 10 carbons is reached, and then decreases. The SmA* phase disappears as the alkyl chain length reaches 10 carbons. The temperature range of the SmC* phase also increases with the chain length.

Table 1. Elemental analysis data for compounds H*n*PBNTP ($n=7$–11).

| | Theory | | Experiment | |
|---|---|---|---|---|
| Compound | C% | H% | C% | H% |
| H7PBNTP | 75.20 | 7.26 | 75.22 | 7.28 |
| H8PBNTP | 75.43 | 7.41 | 74.99 | 7.41 |
| H9PBNTP | 75.64 | 7.56 | 75.51 | 7.56 |
| H10PBNTP | 75.85 | 7.77 | 75.58 | 7.69 |
| H11PBNTP | 76.04 | 7.83 | 75.95 | 7.81 |

Table 2. Transition temperatures (°C) and enthalpies $\Delta H$ (J g$^{-1}$) (in brackets) of chiral compounds H*n*PBNTP ($n=7$–11).

| *n* | I | | SmA* | | SmC* | | Cr | m.p[a] |
|---|---|---|---|---|---|---|---|---|
| 7 | ● | 145.27<br>(5.985) | ● | 120.1<br>(0.128) | ● | 100.4<br>(33.84) | ● | 123.73<br>(40.22) |
| 8 | ● | 142.42<br>(6.831) | ● | 132.54<br>(0.551) | ● | 107.17<br>(39.38) | ● | 129.27<br>(44.27) |
| 9 | ● | 141.06<br>(5.189) | ● | 136.42<br>(0.942) | ● | 112.96<br>(35.63) | ● | 131.59<br>(40.45) |
| 10 | ● | 138.52<br>(8.027) | ● | —<br>— | ● | 113.03<br>(38.82) | ● | 130.77<br>(43.77) |
| 11 | ● | 136.65<br>(8.757) | ● | —<br>— | ● | 109.11<br>(36.37) | ● | 125.69<br>(40.79) |

[a] m.p *refers* to the melting point taken from a DSC thermogram recorded at a heating rate of 5°C min$^{-1}$.

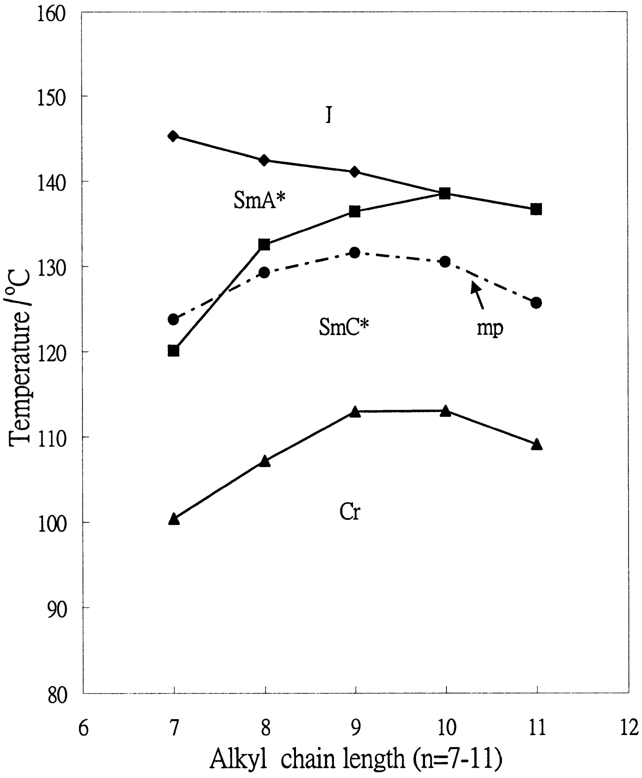

Figure 1. Phase transition temperature versus alkyl chain length $n$ of compounds H*n*PBNTP ($n=7$–11).

### 3.2. *Electro-optical studies*

The switching current behaviour of compound H*n*PBNTP ($n=8$) is shown in figure 2. No switching peak appears in the SmA* phase. A switching current peak appears at 125°C due to the transition from SmA* to SmC*, suggesting the existence of ferroelectricity. As the temperature falls from the transition temperature, the switching current peaks increase slightly.

The spontaneous polarization of the H*n*PBNTP compounds was measured in 5 μm polyimide buffed cells by the triangular wave method [16], the results are shown in figure 3. The spontaneous polarization of these compounds was found to increase with decreasing temperature; the maximum values for H*n*PBNTP ($n=7$–9) are in the range approximate 15–26 nC cm$^{-2}$.

The temperature dependence of the optical tilt angle of the compounds H*n*PBNTP ($n=7$–9) was also measured, with results shown in figure 4. The optical tilt angle increases dramatically as the temperature cooled from the SmA* region to the SmC*. The maximum optical tilt angles $\theta$ are in the range of

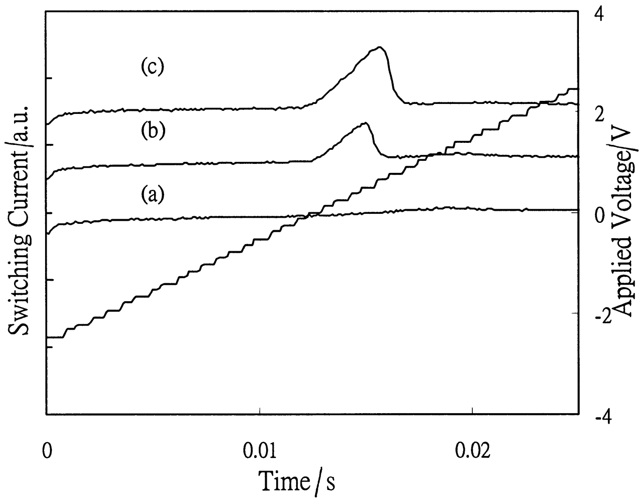

Figure 2. Switching current behaviour of the compound H*n*PBNTP ($n=8$) in the SmA* and SmC* phase at (*a*) 130°C, (*b*) 125°C, (*c*) 110°C.

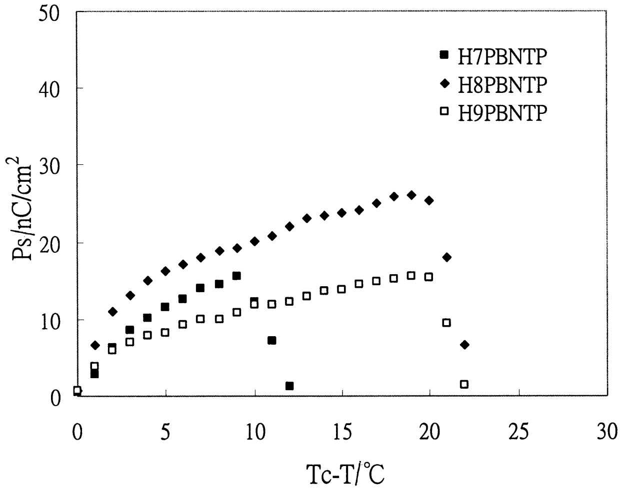

Figure 3. Spontaneous polarization plotted as a function of temperature for H*n*PBNTP ($n=7$–9). $T_c$ is the temperature of the SmA*–SmC* transition.

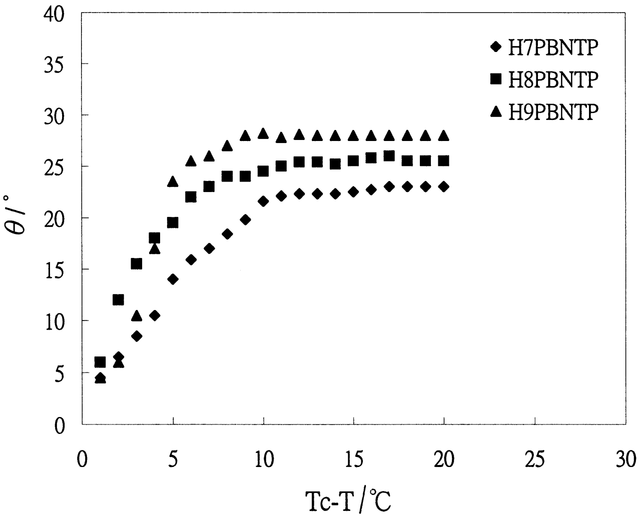

Figure 4. Optical tilt angle plotted as a function of temperature for H*n*PBNTP ($n=7$–9). $T_c$ is the temperature of the SmA*–SmC* transition.

23°–28°. It was clearly shown that the optical tilt angle increases with increasing alkyl chain length.

## 4. Conclusion

A new homologous series of chiral thioesters, hexyl (2*S*)-2-[6-(4-alkanoyloxyphenyl)benzoyloxy-2′-naphthyl] thiopropionates, H*n*PBNTP ($n=7$–11), has been synthesized and was found to exhibit the ferroelectric SmC* phase. These thioester materials favour the formation of chiral tilted smectic phases, and in compounds with longer alkyl chain length ($n=10$ and 11) the SmC* phase is formed exclusively. These results are similar to our previously reported results obtained from the structurally similar chiral thioester materials H*m*PBNTP, except that the thermal stabilities of the mesophases are greater, because the ester group linked to an achiral alkyl chain has higher polarity then the ether group.

The authors are grateful for the financial support of the National Science Council of the Republic of China (NSC 92-2216-E-036-007).

## References

[1] Chandani, A. D. L., Ouchi, Y., Takezoe, H., Fukuda, A., Terashima, K., Furkawa, K., and Kish, A., 1989, *Jpn.J. appl. Phys.*, **28,** 1261.
[2] Yamawaki, M., Yamada, Y., Mori, N., Hayashi, H., Suzuki, Y., Negi, Y. S., Kawamura, T., and Ishibashi, H., 1989, in *Proceedings of the 9th International Display Research Conference,* vol. 3, p. 26.
[3] Yamada, Y., Yamamoto, N., Mori, K., Nakamura, K., Hagiwara, K., Suzuki, Y., Kawamura, T., Orihara, H., and Ishibashi, Y., 1990, *Jpn. J. appl. Phys.*, **29,** 1757.
[4] Johno, M., Chandani, A. D. I., Lee, J., Ouchi, Y., Takezoe, H., Fukuda, A., Itoh, K., and Kitazume, T., 1989, *Proc. Jpn. Display,* p. 22.
[5] Goodby, J. W., Blinc, R., Clark, N. A., Lagerwall, S. T., Osipov, M. A., Pikin, S. R., Sakurai, T., Yoshino, K., and Zeks, B., 1991, *Ferroelectric Liquid Crystals* (USA: Gordon & Breach), pp. 1–97.
[6] Goodby, J. W., and Leslie, T. M., 1984, *Mol. Cryst. liq. Cryst.*, **110,** 205.
[7] Neubert, M. E., Ziemnicka-Merchant, B., Jirousek, M. R., Laskos, J. S., Darrin Leonhardt, J. R., and Sharma, R. B., 1988, *Mol. Cryst. liq. Cryst.*, **154,** 209.
[8] Wu, S.-L., and Hsieh, W.-J., 1996, *Ferroelectrics*, **180,** 259.
[9] Demus, D., and Zaschke, H., 1984, *Flüssige Kristalle in*

*Tabellen* (Leipzig: Deutsher Verlag für Groundstoffindustrie), **3,** 8.

[10] Seed, A. J., Toyne, K. J., Goodby, J. W., and McDonnell, D. G., 1995, *J. mater. Chem*, **5,** 1.

[11] Nguyen, H. T., Rouillon, J. C., Cluzeau, P., Sigaud, G., Destrade, C., and Isaert, N., 1994, *Liq. Cryst.*, **17,** 571.

[12] Nassif, L., Jakli, A., and Seed, A. J., 2001, *Mol. Cryst. liq. Cryst.*, **365,** 171.

[13] Neubert, M. E., Keast, S. S., Ezenyilimba, M. C., Hanlon, C. A., and John, W. C., 1993, *Mol. Cryst. liq. Cryst.*, **237,** 193.

[14] Twieg, R. J., Betterton, K., Nguyen, H. T., Tang, W., and Hinsberg, W., 1989, *Ferroelectrics*, **91,** 243.

[15] Nabor, M. F., Nguyen, H. T., Destrade, C., and Marcerou, J. P., 1991, *Liq. Cryst.*, **10,** 785.

[16] Twieg, R. J., Betterton, K., Hinsberg, W., Wong, P., Tang, W., and Nguyen, H. T., 1991, *Ferroelectrics*, **114,** 295.

[17] Carvalho, P. S., Chaves, M. R., Destrade, C., Nguyen, H. T., and Glogarova, M., 1996, *Liq. Cryst.*, **21,** 31.

[18] Carvalho, P. S., Glogarova, M., Chaves, M. R., Nguyen, H. T., Destrade, C., Rouillon, J. C., Saremento, S., and Ribeiro, M. J., 1996, *Liq. Cryst.*, **21,** 511.

[19] Miyasato, K., Abe, S., Takezoe, H., Fukuda, A., and Kuze, T., 1983, *Jpn. J. appl. Phys.*, **22,** L661.